PERGAMON

Building and Environment 34 (1999) 583–595

BUILDING AND ENVIRONMENT

A two compartment model for determining the contribution of sources, surface deposition and resuspension to air and surface dust concentration levels in occupied rooms

T. Schneider*, J. Kildesø, N.O. Breum

National Institute of Occupational Health, Lersø Parkalle 105, DK 2100, Copenhagen, Denmark

Received 2 September 1997, received in revised form 12 August 1998; accepted 16 September 1998

Abstract

A semi-empirical two-compartment, constant parameter model is used to predict airborne and surface dust concentrations. The model parameters are air in- and exfiltration, internal particle sources, surface deposition caused by settling, Brownian and turbulent diffusion and thermophoresis, track-in of dust particles and resuspension. Model predictions are calculated for some typical scenarios, and the soiling rate of a vertical surface is calculated for a range of friction velocities and electric field strengths. Model sensitivity is determined based on input parameter value distributions for a population of rooms estimated from published data. The predictions are sensitive to track-in and resuspension rates on which field data thus are needed.

1. Introduction

The concentration and composition of dust in the indoor environment are determinants of the indoor environment quality. A large number of factors affect particle concentration in a room, such as the outdoor environment, occupant activities, room design, room properties and physico-chemical properties of particles. Indoor air studies have grappled with these topics [1] and the present work establishes a semi-empirical model for air and surface dust concentration and proposes a method for interpreting the ever increasing amount of field data. In addition, the model can:

(1) facilitate design of cost-effective dust exposure measurement strategies;
(2) support design and implementation of effective dust control strategies based on source reduction, ventilation and cleaning; and
(3) support extrapolation of laboratory scale test results to full scale.

The question immediately arises how to parametrise the model. The modeller will choose model structure, model parameters and output variable depending on the purpose of the model, on the level of understanding of the physics of the candidate parameters, on the existence of sufficient field data on parameter values, on personal preferences, etc. Figure 1 lists some of the many candidate parameters. The primary input parameters are grouped into parameters relating to environment, building and occupants. Some intermediate variables are also shown. It is seen that they may share several input parameters and thus are correlated. The outputs are air and surface concentrations. Figure 1 also illustrates some simple models. Since these models are based on only few parameters they cannot explain all variability in the observed concentrations. One could be misled to think that the more complex a model is made, the better it will be in predicting the observed world. Thus the modeller may be tempted to include an ever increasing number, p, of parameters to improve the predictive power of the model. However, there is a fundamental problem. As stated by [2] in a qualitative way: "It is assumed that the modeller is clever enough that errors in model physics decrease as p increases. Furthermore, the natural or stochastic uncertainty should also decrease as p increases, since more and more of the variability is 'explained' ... The data errors, on the other hand, will increase monotonically with [the number of parameters], whether or not the modeller has chosen the parameters properly." So there is an optimum degree of model complexity that minimises the overall uncertainty.

There is no single model of particle concentrations which is appropriate for all purposes. Following [3] mod-

* Corresponding author. Tel.: 00 45 39 165200; fax: 00 45 39 165201; e-mail: ts@ ami.dk

0360-1323/99/$ - see front matter
PII: S0360-1323(98)00048-1

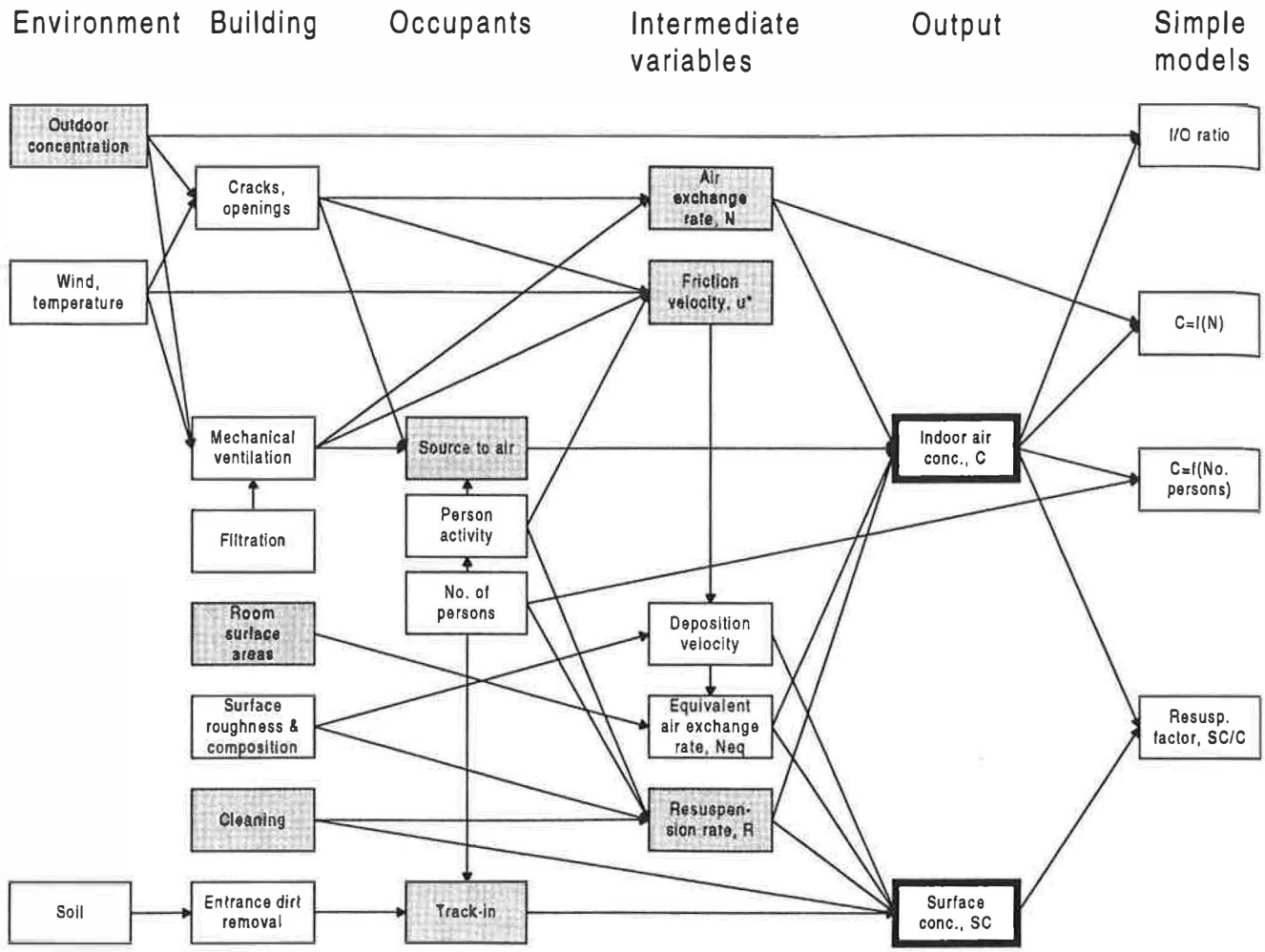

Fig. 1. Diagram showing primary input parameters grouped into parameters relating to environment, building, and occupants and how they a related. Some intermediate variables are also shown. The output are air and surface concentrations. The diagram also illustrates some simple model

els can be classified according to the type of equations used to describe them. The main classes are distributed and lumped parameter models. A model based on Computational Fluid Dynamics (CFD) is an example of the former. CFD calculations require specification of boundary conditions with a level of detail, which is difficult to match by corresponding representative field data. CFD is sensitive to perturbations in boundary conditions, and small deviations between reality and the mathematical model may cause large deviations between the predicted and the observed. If the purpose of modelling is to predict long term averages of particle concentrations in a room with variable source position, a large amount of spatio-temporal averaging must be made of the CFD output.

The other class, the lumped parameter model, conceptually speaking does the averaging first and then the calculation. Lumped parameter compartmental modelling thus is a useful approach to modelling average concentration in a room. Deterministic, linear, multi-compartment models lead to a set of coupled, linear differential equations. For three or more compartments the analytical solutions become very complex an numerical solutions are usually preferred. A review c multi-compartment models for use in indoor air can b found in [4].

Multi-compartment models have been used exte sively, e.g. for studying air quality [5] or airborne partic behaviour [6]. Simpler types of multi-compartme models, the sequential compartment models have bee used [7] for airliner cabin air quality and for predictir solvent concentrations inside storage tanks [8]. The pri ciple that there is a critical number, p, of paramete that should not be exceeded implies that the number compartments has to be limited. Furtaw et al. [9] a others used two air compartments for one room including a virtual compartment surrounding the sourc in order to model the increased concentration close to source. However, even use of only two air compartmen presents some problems since the size and shape of t virtual compartment is somewhat arbitrary, and the are insufficient field data on these parameters and transfer coefficients to and from the remaining co

partments. Raunemaa et al. [10] have studied particle deposition and resuspension using a two compartment model. Thatcher and Layton [11] used a one compartment model, treating the floor as an independent source of particles activated by resuspension.

Nazaroff and Cass [12] have developed a compartmental model for predicting airborne particle concentration and surface deposition velocities onto smooth surfaces. Their model includes ventilation, filtration and aerosol coagulation. Particle deposition on surfaces is calculated for three idealised air flow conditions: homogeneous turbulence, natural and forced convection in combination with thermophoresis and gravitational settling. Particle inertia was neglected and the particle size studied ranged from 0.01 to 2 μm. Nazaroff and Cass [13] used input parameter values that were measured for the specific rooms they modelled. Ligocki et al. [14] used this model to predict surface soiling rates in museums for particle sizes up to 40 μm and modelled the effect of various control strategies.

2. Model

A two compartment model with one air and one surface (floor) compartment will be used to investigate the contribution of outdoor and indoor airborne particle sources, track-in, resuspension and surface deposition on particle concentrations in a room. The build-up of airborne and surface concentrations over 8-h are calculated assuming normal occupant activity. Walls and ceiling are treated as sinks only. It is assumed that the room does not interact with other rooms. Constant parameters are used. Dust removal by cleaning which would represent a quasi-infinite removal rate of very short duration can be modelled as a change in boundary conditions between time slices defined by the cleaning intervals. The model intends to predict room concentrations, not personal exposure. The relation to personal exposure will only be discussed briefly.

The model is applied on some specific scenarios and the model sensitivity is determined. Published data on input parameter values are used to determine the likely distribution of input parameters for a population of rooms. The resulting variability in dust concentration is determined using a probabilistic approach.

The chosen input parameters are highlighted in Fig. 1. The most fundamental model would be based on primary input parameters only. The reason for having included the intermediate variable N (air exchange rate) is that its dependence on primary variables has been studied intensively by others [15]. The dependence of the intermediate variables resuspension rate, R, and friction velocity, u^* (to be defined later), on primary variables is not well understood, and they were used as independent input variables. The limitation of the model is that several input variables such as source rate, resuspension rate and friction velocity are correlated. As an example, high activity levels of room occupants will increase all three.

The mass balance equation written in matrix notation is:

$$\mathrm{d}\mathbf{C}(t)/\mathrm{d}t = A\mathbf{C}(t) + \mathbf{S}(t) \tag{1}$$

$\mathbf{C}$ and $\mathbf{S}$ are the two-dimensional concentration and source vectors, respectively, and A is the system matrix

$$A = \begin{vmatrix} -(N+N_{\mathrm{eq}}) & R/H \\ v_{\mathrm{floor}} & -R \end{vmatrix} \tag{2}$$

where N is the nominal air exchange rate, R is the resuspension rate and H is the room height.
N_{eq} is the equivalent air exchange rate caused by particle removal to surfaces

$$N_{\mathrm{eq}} = \frac{v_{\mathrm{ceiling}} + v_{\mathrm{floor}}}{H} + v_{\mathrm{wall}} \frac{2(L+B)}{LB} \tag{3}$$

where L, B are room length and width and v_{ceiling}, v_{floor}, v_{wall} are particle deposition velocity to horizontal surface facing down (ceiling), facing up (floor) and vertical surfaces (wall).
At equilibrium ($\mathrm{d}\mathbf{C}(t)/\mathrm{d}t = 0$), $\mathbf{C}(\infty) = -\mathbf{A}^{-1}\mathbf{S}$.

The analytical solution of the two coupled differential equations is used. Some preliminary findings using this model approach have been reported previously [16]. In the following, the model structure is described in detail. The model will focus on dust particles in the range 0.1–100 μm. During numerical calculations this range is divided into 200 particle size classes, with class boundaries increasing from 0.1 μm in a geometric progression.

2.1. Sources

Dust particles are introduced into the room air from indoor sources and by outdoor air entering the room at a constant rate, N. Air filtration and recirculation is not considered. The outdoor source term is specified as the concentration of particles in the outdoor air times the penetration factor, P, times the nominal air exchange rate, N.

During normal activities, particles are tracked-in directly to the floor by footwear. These particles constitute a secondary source of airborne particles if they are resuspended by occupant activities [17]. The resuspension process can change the physical property of the particles because agglomeration and deagglomeration take place in the surface compartment and during resuspension. Raunemaa et al. [10] proposed a size modification factor. They used a mass balance approach to determine the total or elemental mass, thereby including the size modification in their results. Another solution could be to consider resuspension as a separate source [18], but this decouples the two compartments. In the present model,

the mass balance equation is formulated for each particle size class separately, and it has to be assumed that there is no exchange of particle mass between size classes. Resuspension from surfaces other than the floor is neglected.

2.2. Sinks

Particles are removed by ventilation. Since a one compartment model is used for the airborne phase, it is implicitly assumed that there is perfect mixing ventilation. It is also assumed that particles are removed with the same effectiveness as the air for the entire particle size range.

The particle removal rate by surface deposition is calculated using a semiempirical model for deposition on smooth surfaces given by [19]. This model is based on homogeneous turbulence and includes particle inertia. Inclusion of inertia is essential, since Nazaroff et al. [20] noted that their (inertialess) model underestimated wall deposition of super micron particles. Use of homogeneous turbulence is in line with Nazaroff and Cass [13] who assumed homogeneous turbulence in a museum with natural ventilation when it was open to the public. The model uses the diffusion equation

$$J = -(D_B + D_\varepsilon)\frac{d\mathbf{C}}{dz} + i|v_e|\mathbf{C} \quad (4)$$

where J is the flux, D_B is the Brownian and D_ε the turbulent diffusion coefficient, $\mathbf{C}$ is concentration at distance z from the wall. v_e is drift velocity induced by external forces (normal to the surface), i is $+1$ or -1 depending on the direction of this force. D_ε is approximated by $D_\varepsilon = k_e z^2$. The solution of eqn (4) is based on the empirically derived relation between particle aerodynamic diameter, stopping distance and friction velocity determined by Sehmel [21]. The friction velocity, u^*, is defined as $u^* = \sqrt{(\tau_0/\rho_{air})}$, where τ_0 is the wall shear stress and ρ_{air} is the density of air. Expressing the turbulence intensity parameter k_e as

$$k_e = a(u^*)^2 \quad (5)$$

and fitting the model to experimental data, gave $a = 0.039\ \mathrm{s\,cm^{-2}}$ and a set of values of u^* corresponding to the set of experimental conditions. Using this model, deposition velocities v_{floor}, v_{wall} and $v_{ceiling}$ are calculated [19].

Nazaroff and Cass [22] included coagulation and thermophoresis. In the present work coagulation is not included, as only low particle concentrations are considered. For the thermophoretic velocity the simple expression is used (see Appendix):

$$v_{thermo} = -0.05 \cdot u^* \cdot K\frac{T_s - T_\infty}{T_\infty} \quad [\mathrm{cm\,s^{-1}}] \quad (6)$$

where K is a constant (see Appendix) and T_s and T_∞ is absolute temperature of surface and of air outside the boundary layer, respectively.

A virtual surface, facing up, is used to calculate potential deposition onto tables, shelves, etc. without entering the mass balance equation.

Some of the deposited particles may become unavailable for resuspension. For outdoor conditions Slinn [23] has modelled this by including a fixation rate parameter in the sink term. In indoor environments such a 'fixation' rate could be caused by the embedment of particles in carpets which would make them unavailable for resuspension, but since no data were available from which a fixation rate could be estimated, fixation is not included in the model. Floor cleaning is a sink which can be handled as a change in boundary conditions for the surface compartment at the time of cleaning.

Surface roughness is an important determinant of deposition velocity. Byrne et al. [24] have in a chamber measured the dependence of deposition velocity on surface roughness, parametrized by the measured friction velocity u^*.

2.3. Charged aerosols

Coulomb and image forces cause a drift velocity of charged particles. Numerical integration of eqn (4) where v_e is determined by image forces showed that the range of image forces is much less than the stopping distance used in the present model at the nominal parameter value and thus can be neglected. In modern buildings, only few surfaces are charged. Thus, Coulomb forces do not significantly affect the mass balance.

The role of Coulomb forces on dust accumulation on surfaces is illustrated by calculating deposition for an aged aerosol (having a Boltzmann equilibrium charge distribution) [25]. The drift velocity, v_e, is

$$v_e = n_p E B_p \quad (7$$

where n_p is number of elementary charges, E is electrical field strength and B_p is particle mobility. The fraction $f(d,n_p)$, of particles of diameter d carrying n_p charges is given by

$$f(d,n_p) = \frac{1}{\sqrt{2\pi}\sigma_d}\exp\left(\frac{-n_p^2}{2\sigma_d^2}\right) \quad (8$$

where $\sigma_d = 2.95\sqrt{d}$, with d in μm [26]. The average deposition velocity for given diameter is obtained by summing over all n_p.

2.4. Output

The mass balance is calculated for each particle size class separately. The mass in each diameter is added to give total airborne concentration, $C_{(Tot)}$, or weighted by

the size conventions [27] to give inhalable, $C_{(Inh)}$, thoracic, $C_{(Tho)}$, and respirable, $C_{(Res)}$, particle concentrations. The 8-h time weighted average concentration, TWA, is also calculated.

Surface dust concentrations, SDC, are calculated both as mass per surface area and as percentage of surface area covered by particle projected area.

In the model the specification of particle size dependent input parameters is based on the aerodynamic diameter. This diameter is transformed to volume equivalent diameter using a density, ρ, and shape factor, χ, that have to be specified. The volume equivalent diameter is used for calculating Brownian diffusion. The volume equivalent diameter is also used for calculating the projected area diameter, and it is assumed that particles deposit without preferred orientation.

The equivalent air exchange rate, N_{eq}, is a convenient intermediate parameter to characterise the average particle removal rate by surface deposition. N_{eq} is calculated for the various size fractions by:

$$N_{eq}(\text{frac}) = \frac{1}{C_{\text{frac}}} \int_d E_{\text{frac}}(x) C(x) N_{eq}(x)\, dx \tag{9}$$

where frac refers to the size fraction (e.g. respirable part of the inhalable fraction), C_{frac} is the aerosol concentration (e.g. respirable) and E_{frac} is the size convention (e.g. respirable fraction).

2.5. Sensitivity

Model sensitivity is the deviation in predicted values for small variations in one or several of the input parameters. Let the model outputs G_j $(j = 1, \ldots, q)$ depend on the input parameter vector $\boldsymbol{\alpha} = (\alpha_1, \ldots, \alpha_p)$. The system function [28].

$$G_j = G_j(\boldsymbol{\alpha})$$

is a function of the parameter vector $\boldsymbol{\alpha}$. Let the nominal parameter vector be denoted $\boldsymbol{\alpha}_0$ and the nominal system function be

$$G_j^0 = G_j(\boldsymbol{\alpha}_0)$$

The sensitivity function is defined as

$$S_{i,j}(\boldsymbol{\alpha}_0) = \left.\frac{\delta G(\boldsymbol{\alpha})}{\delta \alpha_i}\right|_{\alpha_0} \quad (i = 1,2,\ldots,p) \tag{10}$$

The relative parameter induced deviation of output i is:

$$\Delta G_{i,j}(\text{rel}) = \frac{S_{i,j}\Delta\alpha_i}{G_j^0} \tag{11}$$

In order to predict exposure of various populations of room occupants and to recommend generally applicable control strategies the modeller must assess the properties of a population of rooms. Each room is characterised at a given time by a given set of input parameter values. For a population of rooms, the input parameter values form a distribution. The corresponding distribution of predicted values can be estimated using a probabilistic approach [29]. In this approach the input parameter values are described by distributions representing the day to day and between room variability. Uncertainty in the parameter value (which is different from variability) can be included in the distribution. Input parameter values characterising a randomly selected room at a randomly selected day can be considered as one realisation of the stochastic variable $\boldsymbol{\alpha}$. Calculations are performed for a large number of realisations of $\boldsymbol{\alpha}$ (Monte Carlo calculations), where each new realisation is obtained by drawing each input parameter value at random from the corresponding distribution. Covariance between input parameters can be included in the probabilistic approach. The resulting output values describe the distribution of output values characterising the population of rooms and from this distribution confidence intervals can be determined. In the present work a simpler approach is used and only the variance is estimated, not the entire distribution. This is done in terms of error propagation [29]. By making a Taylor expansion of $G(\boldsymbol{\alpha})$ it is seen that the variance of the output can be approximated by

$$\text{Var}(G_j) = \sum_{i=1}^{p} \left(\frac{\partial G_j}{\partial \alpha_i}\right)^2 \text{Var}(\alpha_i) + \sum_{i,r=1(i\neq r)}^{p} \frac{\partial G_j}{\partial \alpha_i}\frac{\partial G_j}{\partial \alpha_r}\text{Cov}(\alpha_i,\alpha_r) \tag{12}$$

where Var is the variance and Cov is the covariance of the input parameter values and provided both are small, i.e. remain within the linear range of the model around $\boldsymbol{\alpha}_0$. The partial coefficient of variations are defined as

$$\text{CV}(G_{i,j}) = \frac{\sqrt{\left(\frac{\partial G_j}{\partial \alpha_i}\right)^2 \text{Var}(\alpha_i)}}{G_j^0} \tag{13a}$$

and the total coefficient of variation as

$$\text{CV}(G_j) = \frac{\sqrt{\text{Var}(G_j)}}{G_j^0} \tag{13b}$$

3. Determination of input parameter distributions

3.1. Principles

If sufficient data are available to generate a reliable distribution of parameter values across a population of rooms the fitted distribution parameters will be used. If very little data are available and all values are positive, Seiler and Alvarez [30] recommend the use of the log-normal distribution with a geometric mean GM and geometric standard deviation GSD estimated as

$$GM = \sqrt{x_{max}x_{min}}; \quad GSD = \left(\frac{x_{max}}{x_{min}}\right)^{1.4} \tag{14}$$

where x_{max} and x_{min} are the largest and lowest value observed for the variable, respectively. Then, if the distribution was indeed log-normal 95% of all observations would be within x_{max} and x_{min}. In some cases *GSD* has to be postulated and the value 3 is used in these cases. This is an arbitrary value, but using the same value at least insures that the contribution to variance is not biased by uncertain differences in *GSD*. The geometric means are used as nominal parameter values, α_i. In the following the background for adopting the distribution parameters (Table 1) is given.

3.2. *Air exchange rate*, N

Wallace [1] quotes 2889 measurements of *N* in homes. The distribution of *N* had geometric mean $GM = 0.46$ h^{-1} and geometric standard deviation $GSD = 2.25$.

3.3. *Internal source rate*, S

Özkaynak et al. [31] determined source strengths in Californian houses, divided into cooking, smoking and 'other sources'. They found that the sum of cooking and 'other sources' contributed 9.7 mg h^{-1}, measured as PM_{10}. For the size parameters chosen (Table 1) the PM_{10} fraction is 77% of the total particles. Thus in terms of total particles, the source strength would be 12 mg h^{-1}, or 3 $\mu g\ s^{-1}$. $GSD = 3$ is postulated.

3.4. *Track-in on floor*, T

Hellstrøm et al. [32] have measured track-in and found values ranging from 0.02 g m^{-2} day^{-1} for a laboratory where shoes were changed to 0.3 g m^{-2} day^{-1} for a post office during dry weather conditions and more than 100 times higher on rainy days. Thatcher and Layton [11] have measured the dust accumulation over 7 days without vacuuming on tracked floor areas in a house. Their results range for 0.011 g m^{-2} day^{-1} (linoleum) to 0.31 g m^{-2} day^{-1} (carpet on ground floor). Since the extreme value occurred on a rainy day the maximum value to be used in eqn (14) was limited to 1 g m^{-2} day^{-1} (10^{-3} g s^{-1} in Table 1).

3.5. *Concentration in air entering room*

There is experimental evidence that the penetration factor, *P*, is one for particles below 10 μm [31] and below 25 μm [11]. In the present model $P = 1$ is used in the entire size range. Thus the concentration, C_{out}, in outdoor air is used for the concentration entering the room. Values of *GM* and *GSD* for particle concentration are postulated.

3.6. *Resuspension rate*, R

Thatcher and Layton [11] determined diameter dependent resuspension rates, *R*, of particles less than 20 μm while four persons performed normal activities on one floor of a house where 40% of the floor area was carpeted. By making a linear regression of the log-transformed values of their data, the parameters *a* and *b* in

Table 1
Geometric mean values *GM* and range or geometric standard deviation, *GSD*, of model parameters

Parameter	Lower bound	Geometric mean	Upper bound	*GSD*	[2]Variance $(0.\ln\alpha_i)^2$
Air exchange rate, *N* [h^{-1}]		0.46		2.25	180
Internal source, *S* [g s^{-1}]		3×10^{-6}		3	783
Track in on floor, *T* [g s^{-1}]	1×10^{-5}	1×10^{-4}	1×10^{-3}	3	783
Concentration in air entering room, C_a [g m^{-3}]		1×10^{-5}		3	783
Resuspension factor, *a*		1.8		2.6	77
Resuspension rate factor, *b* [s^{-1}]		7.2×10^{-10}		3	783
$GM(D_S)$ of internal source size distr. [μm][1]	1.7	4.6	12.4	1.64	35
$GM(D_T)$ of track-in size distr. [μm][1]		50		3	783
$GM(D_{out})$ of outdoor aerosol entering room [μm][1]		1.5		3	783
GSD of all size distributions[1]		2		1	
Friction velocity, u^* [m s^{-1}]	0.01	0.04	0.14	1.9	77
Temperature difference, $T_s - T_x$ [K]	−6	−3	0	—[3]	33[3]

[1] Mass weighted geometric mean aerodynamic diameter, *GM*, and geometric standard deviation *GSD*, of log-normal distribution before truncation
[2] Variance is calculated from *GSD* assuming a log-normal distribution
[3] Variance calculated assuming uniform distribution in the range −6 to 0 K

$R = b^* d_{ae}^a$ [s^{-1}] were determined (Table 1). The correlation was $r^2 = 0.94$. Due to lack of suitable data for $d > 20$ μm, this relation is extrapolated to $d < 100$ μm. As this is far beyond the range of experimental data the values are very uncertain. Thatcher and Layton [11] quote that resuspension rates measured by others could be up to 100 times higher. Hambraeus et al. [33] determined the resuspension factor F = airborne/surface concentration for four persons moving around in an operating suite for 30 min, where the floor had been contaminated with *Staph. aureus*. F was determined from floor concentrations and air concentrations measured after 10 and 25 min after beginning of activity and averaged (seven repeat experiments). The authors stated that the equivalent air exchange rate was 1.9 h^{-1}. Assuming all microorganisms remained viable this would give $d_{ae} = 7$ μm. Inserting these values into the present model the value of b would have to be increased by a factor of 580 to reproduce the measured value of F. If only one person is moving around the increase should be by a factor of 145. Thus the resuspension rate in rooms with high activity and no carpets could be much larger than using the parameter values given in Table 1. It is impossible to arrive at an estimate of GSD of the diameter dependence of resuspension, parametrized by the factor a. The value $GSD = 1.9$ was chosen arbitrarily.

3.7. Size distribution

All size distributions are truncated at 0.1 and at 100 μm and renormalized. Diameter truncation is used to simplify numerical integration over diameters. The lower limit of 0.1 μm is chosen because smaller particles do not contribute to the mass. The upper size limit coincides with the upper limit of definition of the inhalable fraction [27]. The size distribution of the particle sources prior to truncation is assumed to be log-normal with mass weighted geometric mean diameter, $GM(D)$, and geometric standard deviation, $GSD(D)$. All $GSD(D)$ are set equal to 2.

$GM(D_S)$ for internal sources, excluding combustion, is reported to change from 1.7 to 12.4 μm [34]. $GM(D_{out})$ for the outdoor aerosol is postulated.

No size data were available for track-in particles. Since for reasons given above the upper size limit considered was 100 μm the value $GM(D_T) = 50$ μm was chosen quite arbitrarily. The value $GSD = 2$ was used for reasons given.

3.8. Friction velocity, u*

Figure 2 shows experimental deposition velocities onto vertical surfaces from three studies. One set of values was obtained by measuring deposition on wall mounted filter paper in two test houses [35]. Byrne et al. [24] measured deposition velocities in an experimental chamber for two

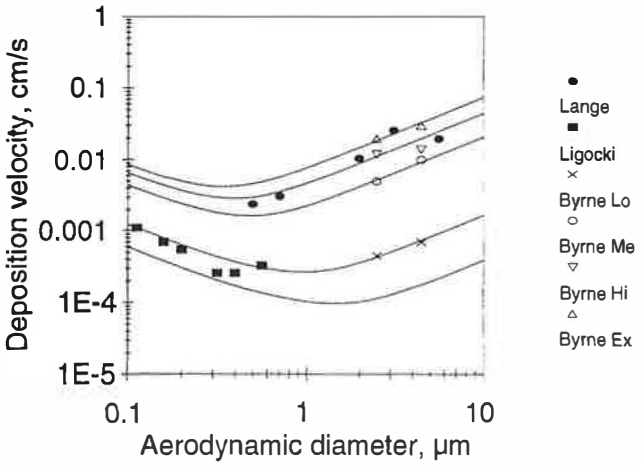

Fig. 2. Experimental deposition velocities and model prediction of wall deposition velocity calculated for the shown friction velocities u^*. Byrne *Lo*, *Me*, *Hi* and *Ex* are the deposition velocities determined by Byrne et al. [24] for low, medium, high and very high friction velocities (aluminium, wallpaper, carpet and Astroturf surface). Lange are deposition velocities on wall mounted filter paper, determined by Lange [35]. Ligocki are deposition velocities determined by Ligocki et al. [14] for a sampling substrate not in thermal contact with the wall. The solid lines are model predictions using (from below) u^* = 1, 2.05, 7.2, 10.5 and 13.5 cm s^{-1}.

particle sizes (2.5 and 4.5 μm) for aluminium, wallpaper, carpet and Astroturf surface. Ligocki et al. [14] measured the deposition velocities of particles onto vertically mounted substrates placed at a wall without thermal contact. Average values from measurements giving the best counting statistics (Sepulveda house) were read from their figures. Model calculations using eqn (4) (no thermophoresis) with values of u^* needed to fit the experimental data are also shown. It is seen that the deposition model explains the diameter dependence. The values of u^* that gave the best fit deviated substantially from the measured values of [24]. Thus there will be an uncertainty regarding the effect of surface roughness on the model predictions. Nevertheless, model predictions using the range in u^* as given in Table 1 would cover the observed range is deposition velocities. The corresponding range for k_e is 0.039–7.6 s^{-1}, which compares favourably with the range of values 0.18–1.9 s^{-1} found for museums [20, 36]. Christoforou et al. [37] measured the deposition velocity on vertical walls in a cave for projected area diameter up to 148 μm. In the range 10–60 μm they also found a linear increase with diameter.

3.9. Thermophoresis

The temperature distribution in the indoor air and on the inner surfaces is complex. A simple scenario will be used. For a wall with a rather poor heat insulation (1.3 W m^{-2} K^{-1}) and an indoor convective heat transfer coefficient of 7.7 W m^{-2} K^{-1} the indoor surface temperature, t_{wall} is estimated from

Table 2
Concentrations for Scenario 1 using average values of the parameter value distributions

Scenario	N_{eq} h^{-1}			TWA [mg m^{-3}]			SDC_{floor} [mg m^{-2}]	SDC_{floor} %	SDC_{shelf} %	$SDC_{ceiling}$ %	SDC_{wall} %
	Tot	*Tho*	*Res*	*Tot*	*Tho*	*Res*					
Scenario 1	1.6	0.58	0.33	0.092	0.080	0.058	98	0.33	0.035	0.000038	0.0019
Floor deposition only	1.6	0.52	0.29	0.095	0.084	0.060	98	0.34	0.035	0.000038	0.0019
Soiling time									13 d	14 y	0.29 y
Scenario 1, inertialess	1.6	0.53	0.30	0.095	0.084	0.060	98	0.34	0.036	0.000017	0.00026
Soiling time									5.6 d	32 y	2.1 y
Scenario 2 (100·b)	47	0.86	0.34	0.14	0.082	0.058	96	0.33	0.26	0.000038	0.0030
Soiling time									0.8 d	14 y	0.18 y

For Scenario 2, b was increased by a factor 100; *Tot*: total fraction, *Tho*: thoracic fraction, *Res*: respirable fraction; y: year, d: day (8 h)

$$t_{wall} = t_\infty - \frac{1.3}{7.7}(t_\infty - t_{outdoor}) \quad (15)$$

It is assumed that this applies for half of the wall area. All other surface temperatures are equal to t_∞. Windows are neglected. For a 1 year period in a temperate zone, $T_s - T_\infty$ would range from -6 to 0 K. For this particular parameter a uniform distribution is assumed.

3.10. Other parameter values

The size of the room is 5×6 ($L \times B$) m^2 and height, H, 3 m. Particle density is assumed to be 1.5 g cm^{-3} and dynamic shape factor 1.25.

4. Results

Calculations have been performed for the following two scenarios, both assuming $T_s - T_\infty = 0$. In Scenario 1, assume that at $t = 0$, the air and all surfaces are particle free. All sources become active at $t = 0$ and last until $t = 8$ h. This scenario would assume daily thorough cleaning of surfaces. For these conditions model predictions using the nominal parameter values have been calculated, Table 2. For the airborne concentrations and N_{eq} the time weighted average is given. For surfaces, the concentration at $t = 8$ h is given. The value of N_{eq} was also calculated, assuming that only floor deposition contributes. To determine the role of particle inertia, the solution of eqn (4) for inertialess particles was also used:

$$v_{wall} = \frac{2}{\pi}\sqrt{k_c D_B} \quad (16)$$

This solution is identical to the equation determined by Corner and Pendlebury [38] and which is used in the model of Nazaroff and Cass [12].

The results are included in Table 2. The deposition velocities to floor, wall and ceiling and the resulting N_{eq} using eqns (4) and (16) are shown in Fig. 3 for $u^* = 0.04$ m s^{-1}.

The sensitivity of each output variable to a +10% change in each of the input variables α_i in turn, $\Delta G_{i,j}$(rel %) is shown in Table 3. For thermophoresis, a zero temperature difference was used as the nominal value, and the 10% change was taken to be -0.6 K. There was no interesting difference between the total and the inhalable airborne particle concentration.

The partial coefficients of variation CV($G_{i,j}$) and the total coefficients of variation CV(G_i) are shown in Table 4. These calculations assumed that there was no covariance between input parameters.

Deposition of an aged aerosol onto surfaces for a range of electric field strength is shown in Fig. 4. The concentration and size distribution corresponded to the 8-h TWA calculated for Scenario 1.

Scenario 2 is the same as Scenario 1, except that resuspension rate, b, is 100 times higher. The results are shown in Table 2.

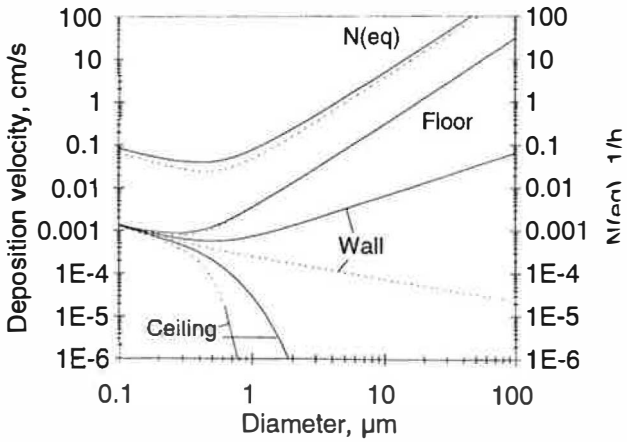

Fig. 3. Deposition velocities on floor, wall and ceiling and the resulting equivalent air exchange rate, $N_{(eq)}$, for $u^* = 0.04$ m s^{-1}. Dashed lines are the result when particle inertia is neglected.

Table 3
Relative (%) deviation of output, $\Delta G_{i,j}$(rel), caused by a +10% deviation in input parameter

	N_{eq} (*Tot*) h^{-1}	N_{eq} (*Tho*) h^{-1}	N_{eq} (*Res*) h^{-1}	*TWA* (*Tot*) mg m^{-3}	*TWA* (*Tho*) mg m^{-3}	*TWA* (*Res*) mg m^{-3}	SDC_{floor} mg m^{-2}	SDC_{floor} % area	SDC_{shelf} % area	$SDC_{ceiling}$ % area	SDC_{wall} % area	$SDC_{coldwall}$ % area
Air exchange, N	3.27	1.42	0.72	−3.41	−3.54	−3.85	−0.04	−0.28	−2.72	−0.22	−3.35	−3.35
Internal source, S	−4.56	0.45	0.53	9.30	9.30	9.08	0.16	0.94	9.05	3.79	9.16	9.16
Track-in, T	5.58	0.05	0.00	0.06	0.00	0.00	9.84	9.03	0.66	0.00	0.06	0.06
Outdoor conc, C_{out}	−0.61	−0.54	−0.57	0.64	0.70	0.92	0.00	0.03	0.29	6.21	0.78	0.78
Resusp. diam. factor, a	61.38	0.36	0.01	0.55	0.01	0.00	−0.02	−0.01	6.88	0.00	0.54	0.54
Resusp. rate factor, b	5.58	0.05	0.00	0.06	0.00	0.00	−0.00	−0.00	0.66	0.00	0.06	0.06
$GM(D_S)$	10.48	10.22	6.14	−6.98	−8.17	−11.64	0.10	−0.10	−0.98	−12.13	−7.27	−7.27
$GM(D_T)$	4.59	−0.08	−0.00	−0.00	−0.00	−0.00	−0.00	−5.96	0.29	−0.00	−0.00	−0.00
$GM(D_{out})$	0.29	0.45	0.64	−0.18	−0.22	−0.40	0.00	0.01	0.10	−14.58	−0.51	−0.51
Friction velocity, u^*	1.43	2.04	2.69	−0.94	−0.94	−0.91	−0.02	−0.09	−0.87	47.51	19.48	19.48
$T_s - T_x$ (−10% change)	0.08	0.13	0.21	−0.05	−0.05	−0.07	−0.00	−0.00	−0.03	−0.16	−0.05	2.92

Table 4
Partial coefficient of variation, $CV(G_{i,j})$ and, bottom row, total coefficient of variation, $CV(G_j)$, all in %

	N_{eq} (*Tot*) h^{-1}	N_{eq} (*Tho*) h^{-1}	N_{eq} (*Res*) h^{-1}	*TWA* (*Tot*) mg m^{-3}	*TWA* (*Tho*) mg m^{-3}	*TWA* (*Res*) mg m^{-3}	SDC_{floor} mg m^{-2}	SDC_{floor} % area	SDC_{shelf} % area	$SDC_{ceiling}$ % area	SDC_{wall} % area	$SDC_{coldwall}$ % area
Air exchange, N	43.8	19.1	9.7	45.7	47.4	51.7	0.5	3.8	36.5	3.0	44.9	44.9
Internal source, S	127.5	12.5	14.9	260.3	260.3	254.1	4.4	26.4	253.3	105.9	256.4	256.4
Track-in, T	156.2	1.4	0.0	1.6	0.1	0.0	275.4	252.6	18.5	0.0	1.6	1.6
Outdoor conc, C_{out}	17.1	15.0	16.1	17.9	19.5	25.7	0.1	0.8	8.0	173.9	21.8	21.8
Resusp. diam. factor, a	538.6	3.2	0.1	4.9	0.1	0.0	0.2	0.1	60.4	0.0	4.8	4.8
Resusp. rate factor, b	156.3	1.5	0.0	1.6	0.1	0.0	0.1	0.0	18.5	0.0	1.6	1.6
$GM(D_S)$	62.0	60.5	36.3	41.3	48.3	68.9	0.6	0.6	5.8	71.7	43.0	43.0
$GM(D_T)$	128.4	2.2	0.1	0.1	0.1	0.0	0.0	166.8	8.1	0.0	0.1	0.1
$GM(D_{out})$	8.2	12.5	17.8	5.1	6.3	11.3	0.1	0.3	2.8	407.9	14.2	14.2
Friction velocity, u^*	12.5	17.9	23.6	8.3	8.3	8.0	0.1	0.8	7.6	416.9	170.9	170.9
$T_s - T_x$	0.5	0.7	1.2	0.3	0.3	0.4	0.0	0.0	0.2	0.9	0.3	16.8
$CV(G_i)$	614.7	70.0	52.6	268.3	269.9	269.9	275.4	303.9	264.7	621.9	315.5	315.9

5. Discussion

5.1. Assumption of complete mixing

Whether the assumption of complete mixing in the air compartment is justified depends on a combination of the following conditions:

(1) While a point source is emitting, a concentration gradient is maintained in the air due to the turbulent diffusion. However, for intermittent sources, the average concentration gradient is reduced as the ratio of on to off periods decreases [39].

(2) The mixing caused by turbulent diffusion in the turbulent core is not instantaneous. Baughman et al. [40] have determined how mixing of a tracer gas released from a point source procceds with time under conditions of natural convection. They defined the characteristic mixing time as the time period required for an instantaneous release from a point source to become uniform to within a relative standard deviation of $<10\%$. For stirring induced by active heating sources and solar load they found characteristic mixing times of less than 15 min. For a typical mechanical ventilation scenario resulting in $N = 1.25\ h^{-1}$, Dreschler et al. [41] found a characteristic mixing time of 7.4 min.

(3) Large particles may have a residence time in the air shorter than the characteristic mixing time. From Fig. 3 it is seen that for particles less than 5 μm, the residence time $1/N_{eq} > 45$ min, thus there will be sufficient time for mixing. For particles larger than 10 μm $1/N_{eq} < 10$ min and there would not be sufficient time for mixing before the particles deposit on the floor. However, a person creates a maximum air velocity of 0.22 m s^{-1} at a distance 0.2 m above the head [42]. This up-current thus may

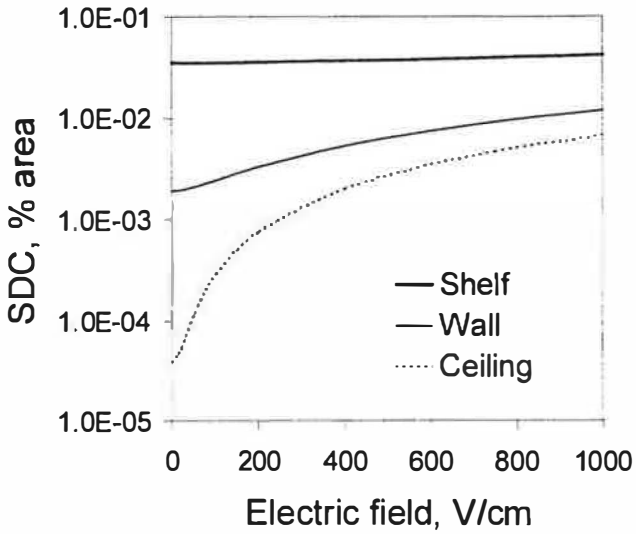

Fig. 4. Effect of electric fields on surface dust accumulation over 8 h for an aged aerosol (Boltzmann charge distribution). Airborne dust concentration corresponds to the 8-h time weighted average determined for Scenario 1.

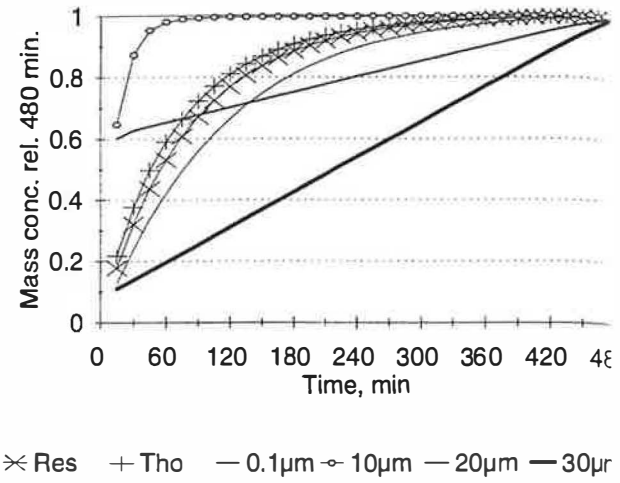

Fig. 5. Time dependent mass concentration in air for Scenario 1, n malised to concentration at $t = 480$ min: Res: respirable fraction, Th thoracic fraction. Also shown are mass concentrations in small diame intervals centred around the stated diameters 0.1, 10, 20 and 30 μm

continuously transport 60 μm particles (settling velocity 0.1 m s^{-1}) or larger to the upper parts of the room from where they settle. Furthermore, the generation of large airborne particles will often coincide with high activity and thus with increased stirring. Field measurements of particle concentration levels in Kindergartens with stationary samplers at height 0.5, 1.1 and 1.7 m above floor with closed face filter holders found no stratification in concentrations [43]. These results suggest that incomplete mixing is not a serious problem for situations corresponding to Scenario 1, but field data are needed on the mixing of non-respirable particles.

The model intends to predict room average airborne concentrations. Concentrations of PM_{10} particulate matter measured by personal samplers was found to be elevated by a factor 1.6 compared with stationary sampling [31]. This increase in particle concentration was dominated by coarse particles (above 2.5 μm), and it was suggested that in part they were particles resuspended from carpets and furniture by motion. It has to be expected, that the present model underestimates the personal 8-h average exposure to airborne particles. If a person on average is far from point sources, then this factor will be at most 1.6.

It is assumed that the floor dust is completely mixed and that resuspension occurs from the entire floor area. However, movements of occupants are usually limited to certain walk areas. The model could be improved by assuming that only a fraction, f, of the floor is walk area and thus participating in the track-in and resuspension process, leaving the $1-f$ floor area fraction as a perfect sink. However, the authors are not aware of data fro which a distribution of f could be estimated.

5.2. Equilibrium

Figure 5 shows the build-up of mass concentration air for Scenario 1 for selected particle size fractions ar for size intervals centred around the shown diameter Calculations were made for Scenario 1 and normalis to concentrations at $t = 480$ min. It is seen that it tak several hours to build up a steady concentration of 0 μm particles. The fastest approach to steady state w obtained for 10 μm particles, but it is much longer tha the residence time (10 min). The increase for much larg particles is almost linear and is caused by the almo linear increase in floor particle concentration during th entire 8-h period. Thus any parameter value derived fro measurements under the assumption of equilibrium questionable.

5.3. Model sensitivity

Table 3 shows that for most outputs the direction change is as would be expected. It is seen that a 10 increase in air exchange rate will reduce surface du concentration of shelves and wall by 3%. For the ceilin the reduction is only 0.2%. This is because an increase N also increases infiltration of the outdoor particles whic are the main contributors to ceiling deposition. Use an un-ducted recirculating air cleaner unit could great reduce the need for cleaning of all surfaces except th floor. The effect of such air cleaners has been studied detail for inertialess particles [13].

The friction velocity, u^*, has a large influence o surface dust concentration, SDC, on walls and ceilin

(Table 3). To further illustrate the role of u^* calculations have been made of SDC_{wall} and $SDC_{ceiling}$ at $t = 8$ h, for Scenario 1, but with u^* ranging from 0.01 to 0.14 m s^{-1} (Fig. 6). Notice the $(u^*)^2$ dependence of SDC_{wall} since for large particles, the deposition velocity onto vertical surfaces given by eqn (4) is proportional to $(u^*)^{2.02}$ [19]. Nazaroff et al. [20] defined the soiling time as the time taken to deposit particles covering 0.2% area. Soiling times have been calculated for Scenario 1 and 2 (Table 2).

Table 4 shows that $SDC_{ceiling}$ is the most highly variable output parameter, and determined by a large number of input variables. It is also seen that variability of some output variables will be explained by one factor (floor concentration in mg m^{-2} is determined by track in rate only), some by two (floor concentration in % area is determined by track in rate and size distribution). The effect of thermophoresis on wall soiling is small compared with other factors. Notice that this result is obtained assuming that the temperature difference is not correlated with u^*.

Table 4 shows that variability in airborne particle concentration across a population of rooms or buildings may be large, as illustrated by CV(G_j). Thus it could be misleading in epidemiological studies to equate exposure of a population of building occupants to airborne dust with the average of measurements in a few rooms. In industrial epidemiology, the term HEG (Homogeneous Exposure Group) has been defined regarding personal exposures as a group of workers with identical probabilities of exposure [44]. The purpose of forming HEGs is to minimise within and maximise between group variance of exposure, and the challenge is to develop grouping criteria. By analogy, a HEG concept should be adopted for indoor air epidemiology. The sensitivity analysis could assist in defining grouping criteria for the building occupants.

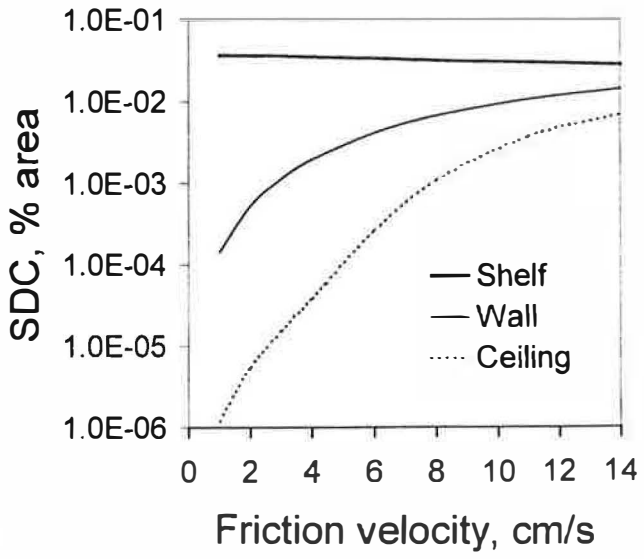

Fig. 6. Surface dust concentration at $t = 8$ h in % area for shelf, wall and ceiling for Scenario 1, but for a range of u^*.

5.4. Comparison with field data

Respirable particle concentrations in an office building had a 95% confidence interval that ranged from 44 to 65 μg m^{-3} [45]. Corresponding mean surface concentration levels ranged from 2 to 3 area % for horizontal surfaces that were close to persons (dusted daily) or easily accessible (dusted weekly), and from 3 to 6 area % for other surfaces (dusted weekly). Thus as a first estimate, surfaces expected to only receive particles from the air accumulate 3–6 area % per week or 0.5–1% per day. Scenario 1 reproduced the measured airborne concentration but greatly underestimated the shelf surface concentration. Scenario 2 (100 times higher resuspension rate) gave a much better fit with the measured value. The model cannot be expected to predict dust concentrations on furniture surfaces close to persons which get contained by occupant activities by other routes than the air as assumed in the present model.

Özkaynak et al. [31] found equivalent air exchange rates of 0.39 h^{-1} for $PM_{2.5}$ and 0.65 h^{-1} for PM_{10}. This is in good agreement with the model prediction as PM_{10} corresponds to the thoracic fraction, and the respirable fraction includes larger particles than the $PM_{2.5}$ fraction. It should be pointed out that N_{eq} is almost only determined by settling to the floor (Table 2).

5.5. General discussion

Figure 2 shows that the deposition model by Schneider et al. [19] provides a consistent interpretation of published results on diameter dependence and of the large differences in deposition velocities. Thus, there is evidence that inertia is an important deposition mechanism in the indoor environment. In terms of dust concentration levels in air and on surfaces, particle inertia is only expected to be of practical relevance for soiling of walls and ceiling (Fig. 3).

Figure 6 shows that rough wall and ceiling surfaces will accumulate much more dust (and e.g. environmental tobacco smoke [46]) than smooth surfaces, but the resulting reduction of airborne dust concentration is negligible. Thus to reduce the risk of odour emission and the need for cleaning, wall and ceiling surfaces should be as smooth as possible. It is interesting to note from Fig. 4 that presence of electric fields always will increase deposition of an aged aerosol.

The floor compartment is less understood than the air compartment and both fixation rates and the mixing process needs to be studied.

A one compartment model cannot handle stratification of large particle concentrations and concentration gradients in the breathing zone. Inclusion of a virtual com-

partment surrounding an occupant could be an improvement. To do this would require field data on parameters characterising this compartment and an approach to take into account that the occupant moves around and resuspends dust from different parts of the floor.

Figure 1, Table 3 and Table 4 provide decision support for selecting suitable parameters to quantify in field studies, and for selecting independent variables in multivariate analysis of dust measurement. The model can be used to check consistency of experimental results.

The sensitivity study has identified which of the model parameters have greatest influence on model predictions. These include track-in and resuspension rates and since only few data exist on diameter dependent resuspension and track-in rates, a considerable part of research on particles in the indoor environment should focus on providing field data on these rates.

Acknowledgements

The authors thank J. Skotte for his support during the programming work.

Appendix

Nazaroff and Cass [22] have estimated the effect of thermophoresis. For the turbulent case they used eqn (4) (without external forces) and substituted the thermal diffusivity, α, for D_B. The solution was

$$v_{thermo} = -fK\frac{T_s - T_x}{T_x} \tag{A1}$$

where T_s is surface temperature, T_x is air temperature outside the boundary layer and K is a constant, see below.

f was found to be

$$f = \frac{v\sqrt{\frac{k_c}{\alpha}}}{\tan^{-1}\left(\delta\sqrt{\frac{k_c}{\alpha}}\right)} \tag{A2}$$

where δ is the thermal boundary layer thickness. The thermophoretic velocity was calculated for the thermal gradient at the surface.

In analogy to the solution of eqn (4) by Schneider et al. [19] an approximation can be made by exploiting that

$$\tan^{-1}\left(\delta\sqrt{\frac{k_c}{\alpha}}\right) \approx \pi/2 \tag{A3}$$

By setting the Prandtl number $v/\alpha = 1$ and using eqn (5) with $a = 0.039$ s cm^{-2}, the approximation used in the present calculations is obtained:

$$f = 0.049\,u^* \tag{A4}$$

Compared with eqn (A2), eqn (A4) was found to underestimate the thermal gradient at the surface by a factor of about 1.7 for $u^* = 0.04$ cm s^{-1}. However, for particles with inertia, it is the thermal gradient at a distance of one stopping distance from the surface which determines the deposition velocity, and at this distance, the thermal gradient has decreased.

According to Talbot et al. [47]

$$K = \frac{2C_s\left(\frac{k_g}{k_p} + 2.2Kn\right) \times \left\{1 + Kn\left[1.2 + 0.041\exp\left(-\frac{0.88}{Kn}\right)\right]\right\}}{(1 + 3C_mKn)\left[1 + \left(2\frac{k_g}{k_p} + 2C_tKn\right)\right]} \tag{A5}$$

Kn is the Knudsen number
k_g, k_p are gas and particle thermal conductivity
$C_s = 1.147$, $C_m = 1.146$, $C = 2.2$

Chomiak and Gupta [48] found that particle rotation in the boundary layer would increase the apparent thermal conductivity of the particle. For the purpose of the present calculations $k_g/k_p = 0.001$.

References

[1] Wallace L. Indoor Particles: A Review. Journal of the Air and Waste Management Association 1996;46:98–126.
[2] Hanna RS. Air quality model evaluation and uncertainty. Journal of the Air Pollution Control Association 1988;38:406–12.
[3] Brogan WL. Modern Control Theory. Englewood Cliffs (New Jersey): Prentice-Hall Inc./Quantum Publishers, Inc., 1982. p. 2–7.
[4] Evans WC. Linear systems, compartmental modeling, and estimability issues in IAQ studies. In: Tichenor BA, editor. Models for Predicting Source and Sink Behavior. ASTM STP 1287, 1996. p. 239–62.
[5] Sandberg M. The multi-chamber theory reconsidered from the viewpoint of air quality studies. Building and Environment 1984;19(4):221–33.
[6] Liao CM, Feddes JJR. Mathematical analysis of a lumped-parameter model for describing the behaviour of airborne dust in animal housing. Applied Mathematical Modelling 1990;14:248–57.
[7] Ryan PB, Spengler JD, Halfpenny PF. Sequential box models for indoor air quality: application to airliner cabin air quality. Atmospheric Environment 1988;22:1031–8.
[8] Haberlin GM, Heinsohn RJ. Predicting solvent concentrations from coating the inside of bulk storage tanks. American Industrial Hygiene Association Journal 1993;54(1):1–9.
[9] Furtaw EJJ, Pandian MD, Nelson DR, Behar JV. Modeling indoor air concentrations near emission sources in imperfectly mixed

rooms. Journal of the Air and Waste Management Association 1996;46:861–8.
[10] Raunemaa T, Kulmala M, Saari H, Olin M, Kulmala MH. Indoor air aerosol model: Transport indoors and deposition of fine and coarse particles. Aerosol Science and Technology 1989;11:11–25.
[11] Thatcher TL, Layton DW. Deposition, resuspension and penetration of particles within a residence. Atmospheric Environment 1995;29:1487–97.
[12] Nazaroff WW, Cass GR. Mathematical modeling of indoor aerosol dynamics. Environmental Science and Technology 1989;23:158–66.
[13] Nazaroff WW, Cass GR. Protecting museum collections from soiling due to the deposition of airborne particles. Atmospheric Environment 1991;25A:841–52.
[14] Ligocki MP, Liu HIH, Cass GR, John W. Measurements of particle deposition rates inside Southern California museums. Aerosol Science and Technology 1990;13:85–101.
[15] Rao J, Haghighat F. A procedure for sensitivity analysis of airflow in multi-zone buildings. Building and Environment 1993;28:53–62.
[16] Schneider T, Kildesø J, Breum NO, Skotte J. Modelling air and surface dust concentration levels. Which parameters are important? In: Yoshizawa S, et al., editors. Proceedings of the seventh International Conference on Indoor Air Quality and Climate. 21–26 July 1996, Nagoya, Japan. vol. 2. Tuesday. p. 447–52.
[17] Sansone EB. Redispersion of indoor surface contamination and its implications. In: Mittal KL, editor. Treatise on Clean Surface Technology. Plenum Publishing Corporation, 1987. p. 261–90.
[18] Ott W, Switzer P, Robinson J. Particle concentrations inside a tavern before and after prohibition of smoking: evaluating the performance on an indoor air quality model. Journal of the Air and Waste Management Association 1996;46:1120–34.
[19] Schneider T, Bohgard M, Gudmundsson A. A semiempirical model for particle deposition onto facial skin and eyes. Role of air-currents and electric fields. Journal of Aerosol Science 1994;25:583–93.
[20] Nazaroff WW, Salmon LG, Cass GR. Concentration and fate of airborne particles in museums. Environmental Science and Technology 1990;24:66–77.
[21] Sehmel GA. Particle deposition from turbulent air flow. Journal of Geophysical Research 1970;75:1766–81.
[22] Nazaroff WW, Cass GR. Mass-transport aspects of pollutant removal at indoor surfaces. Environment International 1989;15:567–84.
[23] Slinn WGN. Formulation and solution of the diffusion-deposition-resuspension problem. Atmospheric Environment 1976;10:763–8.
[24] Byrne MA, Goddard AJH, Lange C, Roed J. Stable tracer aerosol deposition measurements in a test chamber. Journal of Aerosol Science 1995;26:645–53.
[25] Finderup Nielsen N, Schneider T. Particle deposition onto a human head: Influence of electrostatic and wind fields. Bioelectromagnetics 1997;19:246–58.
[26] Reist PC. Introduction to Aerosol Science. London: Macmillan Publishing Company, 1984.
[27] EN 481. Workplace atmospheres—Size fraction definitions for measurements of airborne particles, 1993.
[28] Frank PM. Introduction to System Sensitivity Theory. New York: Academic Press, 1978. p. 7–15.
[29] Haimes YY, Barry T, Lambert JH. When and how can you specify a probability distribution when you don't know much? Risk Analysis 1994;14(5):661–703.
[30] Seiler FA, Alvarez JL. On the selection of distributions for stochastic variables. Risk Analysis 1996;16(1):5–18.
[31] Özkaynak H, Xue J, Spengler J, Wallace L, Pellizzari E, Jenkins P. Personal exposure to airborne particles and metals: results from the particle team study in Riverside, California. Journal of Exposure Analysis and Environmental Epidemiology 1996;6:57–78.
[32] Hellstrøm B, Jahr J, Greger I. Gulvrengjøring (Floor cleaning. In Norwegian). Oslo: Statens bygge og ejendomsdirektorat, 1969.
[33] Hambraeus A, Bengtsson S, Laurell G. Bacterial contamination in a modern operating suite—3: importance of floor contamination as a source of airborne bacteria. Journal of Hygiene, Cambridge 1978;80:169–74.
[34] Owen MK, Ensor DS, Sparks LE. Airborne particle sizes and sources found in indoor air. Atmospheric Environment 1992;26A:2149–62.
[35] Lange C. Indoor deposition and the protective effect of houses against airborne pollution. Report Risø-R-780(EN). Roskilde (Denmark): Risø National Laboratory, 1995.
[36] Nazaroff WW, Ligocki MP, Ma T, Cass GR. Particle deposition in museums: Comparison of modeling and measurement results. Aerosol Science and Technology 1990;13:332–48.
[37] Christoforou CS, Salmon LG, Cass GR. Deposition of atmospheric particles within the Buddhist cave temples at Yungang, China. Atmospheric Environment 1994;28:2081–91.
[38] Corner J, Pendlebury ED. The coagulation and deposition of a stirred aerosol. Proceedings of the Physical Society London 1951;B64:645–54.
[39] Mage DT, Ott WR. Accounting for nonuniform mixing and human exposure in indoor environments. In: Tichenor AB, editor. Models for Predicting Source and Sink Behavior. ASTM STP 1287, 1996. p. 263–78.
[40] Baughman AV, Gadgil AJ, Nazaroff WW. Mixing a point source pollutant by natural convection flow within a room. Indoor Air 1994;4:114–22.
[41] Dreschler AC, Lobascio C, Gadgil AJ, Nazaroff WW. Mixing of a point-source indoor pollutant by forced convection. Indoor Air 1995;5:204–14.
[42] Homma H, Yakiyama M. Examination of free convection around occupant's body caused by its metabolic heat. ASHRAE Transactions 1988;44:104–24.
[43] Rindel A, Bach E, Breum NO, Hugod C, Nielsen A, Schneider T, TSQ. Mineraluldslofter i børnehaver, Arbejdsmiljø fondet, København, 1985.
[44] Hawkins NC, Norwood SK, Rock JC. A strategy for occupational exposure assessment. American Industrial Hygiene Association, Akron, Ohio, 1991.
[45] Kildesø J, Tornvig L, Skov P, Schneider T. An intervention study of the effect of improved cleaning methods on dust concentration and on dust composition. Indoor Air 1998;8:12–22.
[46] Bluyssen P, Vandeloo H, Leaderer BP. Chamber and field studies of respirable suspended particulate deposition rates indoors. Indoor Air '87. Proceedings of the fourth International Conference on Indoor Air Quality and Climate, Berlin 17–21 August 1987. vol. 1. Institute for Water, Soil and Air Hygiene, Berlin, 1987. p. 549–53.
[47] Talbot L, Cheng RK, Schefer RW, Willis DR. Thermophoresis of particles in a heated boundary layer. Journal of Fluid Mechanics 1980;101:737–58.
[48] Chomiak J, Gupta AS. Thermphoresis in boundary layer flows. Journal of Aerosol Science 1989;20:1–5.